Eurasia Journal of Science and Technology
ISSN: 2663-1016
DOI: https://doi.org/10.61784/ejst3078

PERFORMANCE COMPARISON OF FREE-PISTON STIRLING CRYOCOOLERS WITH METALLIC AND NON-METALLIC PACKING IN WOUND REGENERATORS

ShuLing Guo, AnKuo Zhang*
Department of Refrigeration and Cryogenic Engineering, Shanghai Ocean University, Shanghai 201306, China.
Corresponding Author: AnKuo Zhang, Email: zhangankuo@126.com

Abstract: In recent years, cryogenic technology has undergone continuous advancement. Compared with traditional multi-stage cascade vapor-compression cryocoolers, Stirling cryocoolers exhibit advantages such as compact structure, high reliability, and low environmental pollution, thus garnering significant attention from researchers. The regenerator, being the most costly component within Stirling cryocoolers, can see substantial production cost reductions through optimization of regenerator packing materials. Wound regenerators, owing to their compatibility with mechanical winding processes, eliminate material waste during fabrication. This approach significantly reduces both labor and material costs compared to stacked wire mesh regenerators, positioning wound configurations as a promising solution for cost-effective regenerator design. This study systematically investigates the internal losses, working characteristics, and refrigeration performance of a free-piston Stirling cryocooler prototype featuring wound regenerators. Experimental results demonstrate that at an operating temperature of 187 K, the Stirling cryocooler with non-metallic regenerator packing achieved a cooling capacity of 280 W, outperforming its metallic counterpart 180 W. Furthermore, the non-metallic variant exhibited a COP 0.2 higher than the metallic regenerator system, conclusively establishing the superior thermodynamic performance of non-metallic packing in wound regenerators.
Keywords: Heat transfer; Cryogenic; Stirling cryocooler; Cooling efficiency

1 INTRODUCTION

In recent years, cryogenic technology has continuously developed. Small Stirling cryocoolers have been widely applied in fields such as low-temperature storage. Compared with traditional multi-stage cascade cryocoolers, Stirling cryocoolers have more environmentally friendly working fluids and simpler, more efficient systems, thus being highly favored[1]. Among them, free-piston Stirling cryocoolers use linear motors to replace the traditional crankshaft-connecting rod drive structures and employ flexure springs and gas bearing technology for support, possessing advantages of low noise, small vibration, and higher compactness. Since their inception, they have received extensive attention from researchers[2-3].

Due to limitations in production costs and technical costs, Stirling cryocoolers were initially mainly used in aerospace and infrared detection fields. With the continuous maturation of Stirling refrigeration technology, the applications of Stirling cryocoolers have begun to expand. In the past decade, Stirling cryocoolers oriented toward general consumers have become a new direction of research. As a regenerative cryocooler, the regenerator is a critical component affecting the refrigeration performance of Stirling cryocoolers. The packing methods and parameters of regenerator packings have a direct impact on the regenerator's performance. Selecting appropriate packing materials is crucial for the overall system performance of the cryocooler[4]. Meanwhile, the regenerator is also one of the most expensive components in Stirling cryocoolers. Therefore, to reduce the manufacturing costs of Stirling cryocoolers, optimization of regenerator packing can be implemented[5]. Currently, stacked wire-mesh is the most commonly used packing method for Stirling cryocooler regenerators. This type of regenerator possesses high specific surface area and volumetric heat capacity, along with low axial thermal conductivity. However, it suffers from disadvantages such as metal material waste and complex manufacturing processes. The production process of stacked wire-mesh regenerators requires cutting square wire-mesh into annular components needed for packing, which wastes significant material. Additionally, manually packing the wire-mesh into the regenerator substantially increases labor costs. In contrast, wound wire-mesh structures can utilize automated mechanical winding processes, enabling drastic reductions in both labor costs and material costs, thereby serving as an effective solution for lowering regenerator costs.

Currently, research targeting wound wire mesh regenerators remains relatively limited. Wound wire mesh can be categorized into metallic and non-metallic types based on material differences. Metallic wire-mesh is typically fabricated from stainless steel. The Technical Institute of Physics and Chemistry, Chinese Academy of Sciences experimentally compared spiral-wound metallic wire-mesh with traditional stacked metallic wire-mesh. Results demonstrated that compared to stacked wire-mesh, spiral-wound configurations achieved over 80% reduction in both manufacturing costs and processing time. While stacked wire-mesh regenerator cryocoolers exhibit superior refrigeration efficiency, spiral-wound variants demonstrate lower flow resistance with efficiency comparable to vapor-compression refrigeration systems, showing promising application potential in deep-cryogenic cooling performance.Non-metallic wire-mesh is generally fabricated by winding polyester films[6]. Zhu Haifeng et al. investigated the use of PET fibers as a metallic substitute for regenerator packing, with the input PV power increasing

by only 5W at 1W@80K operating conditions, demonstrating the feasibility of replacing metallic materials with non-metallic alternatives in regenerator packing[7]. Cui Yunhao et al. conducted comparative performance tests on regenerators employing random stainless steel wire-mesh packing versus polyimide film spiral-wound packing. Results demonstrated that the spiral-wound non-metallic wire-mesh regenerator exhibited a 16% higher relative Carnot efficiency compared with the randomly packed stainless steel wire-mesh regenerator[8].

Wound wire mesh regenerators exhibit distinct performance variations in cryocoolers depending on their material composition. This study investigates the operational differences in cryocoolers caused by metallic versus non-metallic materials under identical packing configurations through numerical simulations and experimental validation. Based on a prototype free-piston Stirling cryocooler, a comprehensive Sage model of the entire refrigeration system was established. Comparative analyses were conducted on temperature distributions, internal loss characteristics, and their spatial profiles across regenerators with different materials. The research systematically examines the impacts of packing parameters and operational variables on refrigeration efficiency, while determining optimal packing specifications, operating frequencies, and charge pressures. Predictive simulations and performance comparisons were executed for both metallic and non-metallic regenerator configurations.

2 NUMERICAL CALCULATION

To investigate the performance differences between free-piston Stirling cryocoolers with metallic versus non-metallic spiral-wound regenerators, this study employs the one-dimensional cryocooler modeling software Sage for computational analysis. The software numerically solves the governing equations of mass, energy, and momentum conservation through finite difference method to obtain simulation results. Sage utilizes graphical interface-based modeling, constructing system-level simulations by defining dimensional parameters, geometric configurations, and material properties of individual cryocooler components. These components are interconnected through mass flow dynamics, pressure wave propagation, mechanical forces, and energy transfer pathways, thus enabling comprehensive system-level simulation and performance optimization.

2.1 Thermodynamic Analysis of Free-Piston Stirling Cryocooler

The free piston Stirling cooler is a closed system. Under the drive of the motor, the input power obtained by the compression piston is $\dot{W}$; gas working fluid releases heat to the external environment, with a heat release of $\dot{Q}_1$; the gas working fluid drives the movement of the exhaust device, and the amount of work done to the exhaust device is $\dot{W}_0$; at the expansion chamber, the gas working fluid absorbs heat from the cold source, producing a cooling capacity of $\dot{Q}_0$.The external ambient temperature is T_1. The cold end temperature is T_0.

For a free piston Stirling cooler, the first and second laws of thermodynamics can be expressed as:

$$\dot{W} - \dot{W}_0 = \dot{Q}_1 - \dot{Q}_0 + \frac{d(mu)}{dt} \tag{1}$$

$$\frac{\dot{Q}_1}{T_1} - \frac{\dot{Q}_0}{T_0} + \dot{S}_{ex} = \frac{d(mt)}{dt} \tag{2}$$

where, $\frac{d(ms)}{dt}$ is the rate of change of internal energy in the refrigeration system, $\frac{d(mt)}{dt}$ is The rate of change of entropy in the refrigeration system is 0 in steady state.

By combining the above equations, the COP of the refrigeration unit can be obtained as[9]:

$$\mathrm{COP} = \frac{\dot{Q}_0}{\dot{W} - \dot{W}_0} = \frac{T_0}{T_1 - T_0}\left[1 - \frac{T_0 \dot{S}_{ex}}{\dot{W} - \dot{W}_0}\right] \tag{3}$$

2.2 Numerical Calculation

Within the numerical model, the one-dimensional governing equations of momentum, continuity, and energy within the gas domain are as follows:

$$\frac{\partial \rho A}{\partial t} + \frac{\partial \rho u A}{\partial x} = 0 \tag{4}$$

$$\frac{\partial \rho u A}{\partial t} + \frac{\partial u \rho u A}{\partial x} + \frac{\partial P}{\partial x} A - F A = 0 \tag{5}$$

$$\frac{\partial \rho e A}{\partial t} + P\frac{\partial A}{\partial t} + \frac{\partial}{\partial x}(u \rho e A + u P A + q) - Q_w = 0 \tag{6}$$

where P, u, A and ρ denote the working gas pressure, mean-flow velocity in the x direction (longitudinal), cross sectional area and working gas density, respectively[10].

Due to non-ideal factors, there are a series of losses within the FPSC that affect its refrigeration efficiency. The losses of the cryocooler are divided into static losses and dynamic losses. Static loss is mainly heat conduction loss.

The axial heat conduction loss caused by heat conduction can be solved based on Fourier's law:

$$Q_{con} = -\lambda A \frac{dT}{dx} \tag{7}$$

Dynamic losses are typically the most significant losses during the operation of a cryocooler. Dynamic losses of a cryocooler include incomplete heat exchange losses, pressure drop losses, and leakage losses.

In an ideal regenerator, heat exchange between the packings and the working fluid is highly efficient. However, in actual operation, due to the temperature difference between the gas flow and the regenerator, there is an insufficient heat exchange phenomenon, resulting in non-ideal heat transfer losses. The non-ideal heat transfer losses Q_r can be calculated as follows:

$$Q_r = \dot{m}_r c_p (1-\eta)(T_{cr} - T_{er}) \tag{8}$$

where $\dot{m}_r$ is the average mass flow rate of gas through the regenerator during the cold and hot blow periods, c_p is the average specific heat capacity at constant pressure of the working fluid, and T_{cr}, T_{er} are the temperature at the cold and hot ends of the regenerator.

The flow resistance inherent in cryocooler operation induces amplitude attenuation of the working fluid's oscillatory flow, consequently generating flow resistance losses. The definition of pressure drop loss Q_f is as follows:

$$Q_f = \oint \Delta P_r dV_e \tag{9}$$

where ΔP_r is the pressure drop across the regenerator, and V_e is the volume of the expansion volume.

Flow resistance losses mainly occurs in the regenerator part of the cryocooler. The pressure drop ΔP_r in the regenerator is as follows:

$$\Delta P_r = \frac{f_r G_r{}^2 L_r}{2 K_{ci} R_{Mr} \rho_{Mr}} \tag{10}$$

where C_f is the friction factor, G_r is the mass flow rate per unit flow area, L_r is the length of the flow path, K_{ci} is the unit conversion coefficient, and R_{Mr} is the hydraulic radius of the flow path.

2.2 Regenerator Material Property Comparison

The regenerator is the core component enabling work-heat conversion. Alternating fluid and solid packing continuously undergo heat exchange within the regenerator, thus the selection of regenerator packing must satisfy thermophysical property requirements. The volumetric heat capacity of regenerator packing should be significantly greater than that of the working gas[2]; large heat transfer area ensures sufficient heat exchange between gas and packing; low flow resistance reduces working fluid flow losses; small axial thermal conductivity decreases cold-end heat losses. While packing structures simultaneously satisfying all these characteristics are difficult to achieve, appropriate regenerator packing can be selected based on specific application requirements. Among them, spiral-wound regenerators feature simple structures and lower manufacturing costs. The structural diagram and physical diagram of the spiral-wound regenerator are shown in Figure 1。

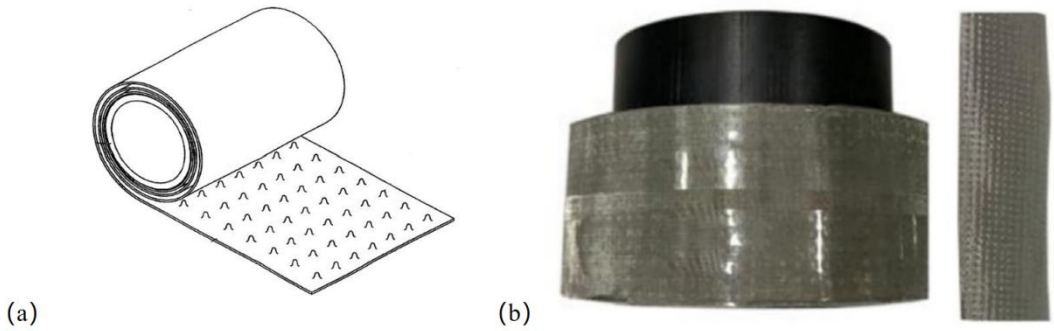

Figure 1 Non-Metallic wound Regenerator Structural Diagram (a) and Physical Diagram of Metallic wound Regenerator Packing (b) [6]

Wound regenerator packing is categorized into metallic and non-metallic types. Metallic packing typically employs 304 stainless steel. Non-metallic packing commonly utilizes polyester materials such as polyester (PET), PEN, Teflon, and polyimide. Due to material properties, stainless steel regenerators exhibit significantly higher axial thermal conductivity than non-metallic materials, resulting in greater axial heat losses within the regenerator. However, stainless steel demonstrates superior volumetric specific heat capacity compared to non-metallic materials, endowing it with enhanced thermal energy storage capabilities. At 100K, the volumetric specific heat of helium is approximately 0.86 J/(m³·K), significantly lower than that of both regenerator packing materials. Therefore, both material types can be effectively utilized for heat exchange in regenerators (Figure 2).

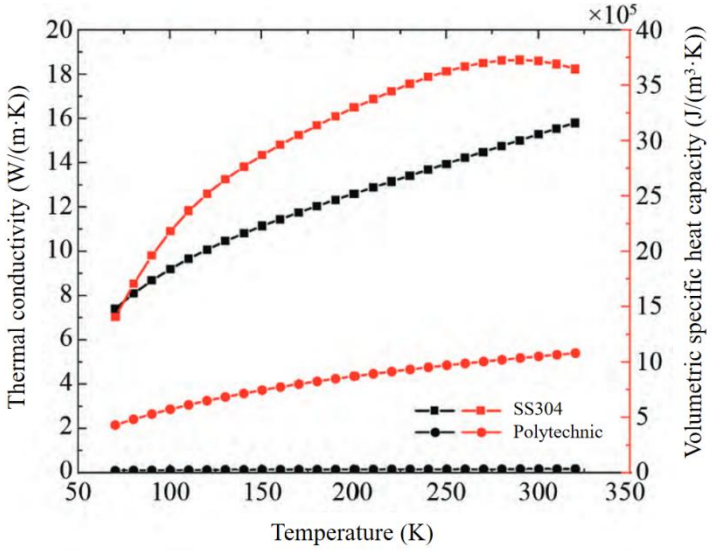

Figure 2 Comparison of Thermal Conductivity and Volumetric Heat Capacity between Polyimide and 304 Stainless Steel as Functions of Temperature[8]

The spiral-wound metallic packing is typically fabricated by winding metallic wire mesh, featuring a more porous and loose structure that provides a larger specific surface area. In contrast, non-metallic polyester films usually employ perforated surfaces, resulting in relatively lower porosity and smaller specific surface area. In Stirling cryocoolers, the regenerator generally reciprocates with the displacer within the expansion cylinder. A greater mass leads to increased mechanical vibration during operation, necessitating higher radial stiffness in the flexure springs[8]. Excessive vibration and friction can also reduce the operational lifespan of the cryocooler. Non-metallic materials, being lighter than their metallic counterparts, can decrease the regenerator mass and mitigate vibration-related issues. The flow channels in spiral-wound regenerators are parallel and well-ordered, ensuring relatively low flow resistance for both metallic and non-metallic materials.

Compared with metallic packing, non-metallic packing has significantly lower costs. Taking PEN material as an example, the material cost for spiral-wound PEN is only 5% of that for 200-mesh wire mesh, with processing and filling costs also being lower than those for metallic wire mesh. The total production cost of PEN material regenerators is approximately 16% of that for metallic materials (Table 1).

Table 1 Total Cost Estimation of Metallic and Non-Metallic Packing for Wound Regenerators

Mateiral	Wound PEN material	Wound 200 mesh metal wire mesh
Raw material cost/USD	0.7	13.8
Processing and filling costs/USD	2.1	2.8
Total cost/USD	2.8	16.6

3 SIMULATION SETUP

To further analyze the differences between metallic and non-metallic packing regenerators, this study employs one-dimensional simulation software to model two distinct cryocooler configurations. Concurrently, an experimental platform was established to validate both the simulation results and the actual performance of the two cryocooler types. This section details the model configuration and experimental apparatus specifications.

The schematic diagram of the prototype used for experimental research in this study is shown in the figure below. This free-piston Stirling cryocooler primarily consists of the following components: cold head, cold-end heat exchanger, regenerator, hot-end heat exchanger, displacer piston, compression piston, linear motor, flexure springs, and vibration damping device. The low-temperature cooler generates an alternating magnetic field by using a high-frequency AC power source to drive the reciprocating motion of the compression piston.This movement forces the helium working fluid to produce a cooling effect through the cold fingers. In addition, a vibration reduction device is installed at one end of the system to effectively reduce vibration and noise. For the metallic packing regenerator, it is fabricated by spirally winding strip-shaped SS304 stainless steel wire mesh, with porosity adjusted through mesh protrusions. The non-metallic packing utilizes PEN film, which is first perforated on its surface and then wound into shape (Figure 3).

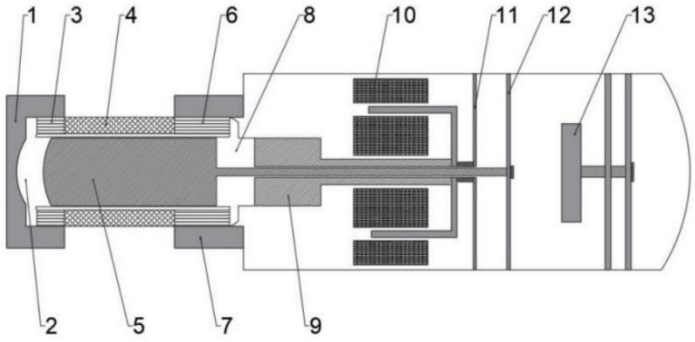

1.cold head; 2.expansion volume; 3.cold heat exchanger; 4.regenerator; 5.displacer; 6.hot heat exchanger; 7.hot heat radiator; 8.compression volume; 9.compression piston; 10.linear motor; 11.compression flexure bearing; 12.displacer flexure bearing; 13.vibration damping device

Figure 3 Structural Diagram of Free-Piston Stirling Cryocooler

In the model, the cryocooler operates at a working frequency of 55 Hz with a charge pressure of 3.0 MPa, using helium as the refrigerant. The external environment of the refrigerant is set to 310 K. Since the cryocooler primarily serves as the cold source for a low-temperature refrigerator, the cold-end temperature is set to 187 K.

4 RESULTS AND DISCUSSION

4.1 Axial Temperature Distribution along the Entire Cryocooler with Metallic Versus Non-Metallic Packing Regenerators

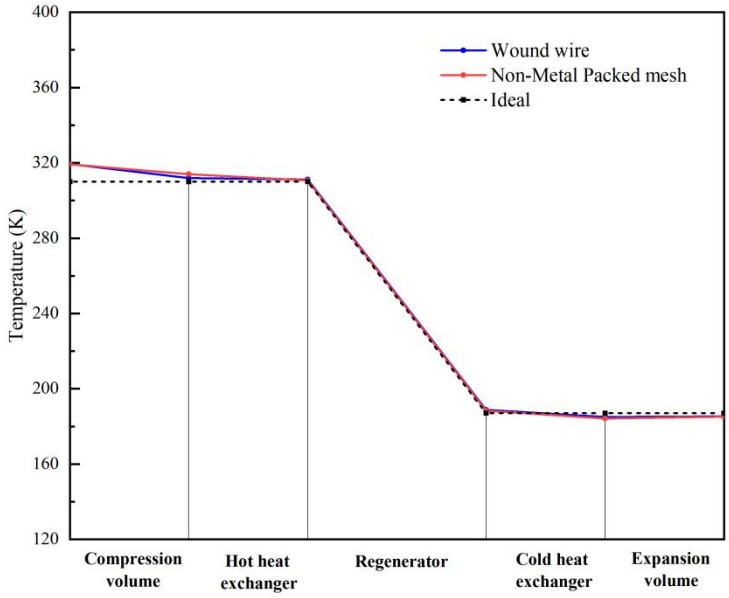

Figure 4 Axial Temperature Distribution Diagram of Complete Cryocooler with Metallic vs. Non-Metallic Packing

Figure 4 shows the axial temperature distribution from the compression chamber inlet to the expansion chamber outlet comparing the actual internal temperatures of Stirling cryocoolers with metallic and non-metallic regenerators against the theoretical temperature distribution. In the compression chamber, the actual internal temperature of the cryocooler is higher than the ideal temperature. This occurs because the ideal cryocooler process assumes isothermal compression, whereas the actual cryocooler undergoes near-adiabatic compression, resulting in significantly higher gas temperatures at the compression chamber end compared to theoretical values. From the compressor to the hot-end heat exchanger outlet, the cryocooler temperature continuously decreases. Before the gas reaches the hot end of the regenerator, its temperature remains higher than the ideal temperature, with the non-metallic regenerator cryocooler showing even higher temperatures in the compression chamber. In the hot-end heat exchanger, the temperature decrease rate slows down. Within the regenerator, the temperature drops rapidly, with both cryocooler types showing good agreement with the ideal temperature drop rate. At the cold-end heat exchanger, the actual gas temperature decreases slightly, with both cryocooler types exhibiting similar temperatures. From the expansion chamber inlet to outlet, the actual cryocooler

temperature rises slightly because the working gas absorbs heat during expansion, causing a minor temperature drop at the expansion chamber outlet. Both cryocooler configurations show essentially identical temperature distributions from the cold-end heat exchanger inlet to the expansion chamber outlet.

4.2 Impact of Regenerator Parameters on Cooling Efficiency in Cryocoolers with Metallic Versus Non-Metallic Packing

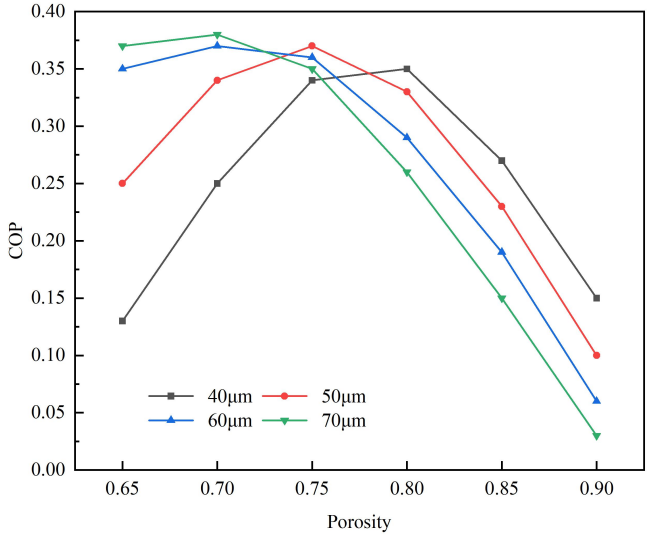

Figure 5 The Relationship between Porosity and COP of Wound Wire Mesh Stirling Cryocooler Regenerators at Different Wire Diameters

For metallic regenerators, the wire diameter of the metal mesh and the porosity of the packing are the main regenerator parameters. Figure 5 shows the relationship between porosity and COP for metallic regenerators with different wire diameters. In the 40-70 μm wire diameter range, COP first increases and then decreases as porosity increases. This is because when the wire diameter is fixed, at lower porosity levels, increasing porosity creates more voids between the metal materials, allowing smoother gas flow and reduced flow resistance while maintaining sufficient effective heat transfer area. This enables more efficient heat exchange between the gas and metal materials, improving the regenerator's heat transfer performance and thereby increasing the cryocooler's COP. However, when porosity exceeds a certain value, the proportion of metal material decreases, meaning the effective surface area available for heat exchange is reduced. With fewer contact opportunities between the gas and metal materials, heat exchange becomes insufficient, incomplete heat transfer losses increase, leading to degraded cryocooler performance and lower COP.

The porosity corresponding to maximum COP shifts toward lower values as wire diameter increases. This occurs because larger wire diameters result in greater actual metal volume fraction within the same space. Consequently, sufficient metal surface area for heat exchange can be maintained even at lower porosity levels. Compared with fine wires, excessively high porosity becomes unnecessary for preserving effective heat transfer area; simultaneously, thicker wires make gas flow channels relatively narrower and more complex within the regenerator. At higher porosity, although gas flow space increases, the coarser wires cause more significant flow resistance due to enhanced flow disturbances and friction in the channels. Therefore, for thicker wires, relatively lower porosity optimizes gas flow conditions, achieving better balance between flow resistance and heat transfer effectiveness, thus maximizing COP at reduced porosity levels. The maximum COP occurs at 70μm wire diameter. Peak COP values appear at 70μm/0.7 porosity, followed by 60μm/0.7 and 50μm/0.75 combinations.

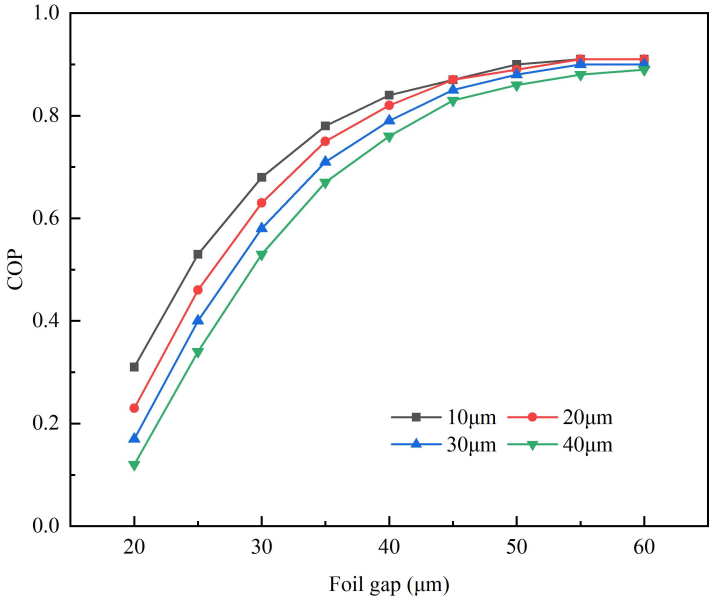

Figure 6 The Relationship between the Foil Gap and the COP of the Regenerator in a Wound Non-Metallic Stirling Cryocooler under Different Foil Thicknesses

The primary regenerator parameters for non-metallic regenerators are foil thickness and foil gap. Figure 6 presents the relationship between foil gap and COP for non-metallic regenerators under varying foil thicknesses. Unlike metallic regenerators, within the 10-40 μm foil thickness range, COP increases with growing foil gap until stabilizing after reaching 45 μm gap. At smaller gaps, confined gas flow channels result in significant flow resistance losses that impair cooling efficiency. Consequently, COP shows marked improvement with increased gap. However, excessive gap reduces gas-packing heat exchange effectiveness, causing substantial incomplete heat transfer losses. When gap exceeds 45 μm, these losses outweigh flow resistance effects on cooling efficiency, leading to stabilized COP growth. Maximum COP values consistently occur at 55 μm gap across all thicknesses.

Within the 10μm-40μm foil gap range, the influence of increasing foil thickness on COP remains relatively minor. As foil thickness grows, the maximum COP shows slight decrease, though all configurations achieve similar peak COP values. The absolute maximum COP occurs at 20μm foil thickness with 55μm gap.

4.3 Impact of Working Parameters on Cooling Efficiency in Cryocoolers with Metallic Versus Non-Metallic Packing Regenerators

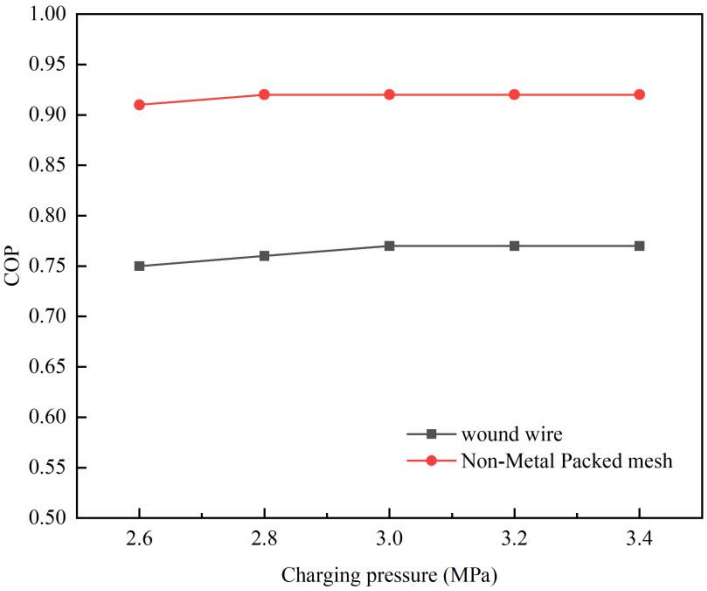

Figure 7 Comparison of Charging Pressure and COP in Metallic and Non-Metallic Cryocoolers

Figure 7 shows the variation of Stirling refrigerators with different material recuperators under different inflation

pressures. COP increases with rising charge pressure, exhibiting a higher growth rate below 3.0 MPa before stabilizing beyond this point. The maximum COP of 0.77 is attained within the 3.0-3.4 MPa range, with no significant further increase thereafter. This occurs because increased charge pressure enables higher compressor input power at identical piston stroke while simultaneously increasing working gas density, which enhances volumetric heat capacity and refrigeration capacity per cycle during expansion, thereby boosting PV work, theoretical refrigeration capacity and COP. However, as charge pressure continues to rise, refrigeration losses progressively increase. When the incremental gain in theoretical refrigeration capacity approaches the total loss increase, COP stabilizes at its maximum value. At charge pressures below 2.6 MPa, the lower COP indicates severely constrained cryocooler performance due to insufficient pressure.

The observed COP variation pattern primarily stems from elevated charge pressure increasing gas density, which alters heat transfer characteristics between the gas and regenerator packing under isothermal conditions. This exacerbates insufficient heat transfer, resulting in inadequate thermal exchange that amplifies incomplete heat transfer losses. Concurrently, the increased gas density and viscosity under higher charge pressure amplify flow resistance within the regenerator channels, intensifying flow resistance losses. Thermal conduction losses show minimal variation compared to flow resistance and incomplete heat transfer losses.

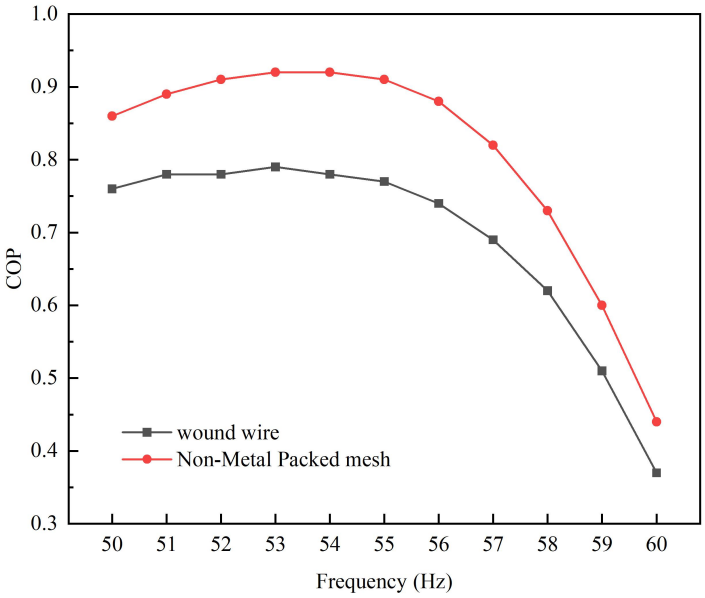

Figure 8 Comparison of the Relationship between the Working Frequency and COP of the Metallic and Non-Metallic Packing Regenerator Cryocoolers

Figure 8 presents a comparison of the relationship between operating frequency and COP for metallic and non-metallic regenerator cryocoolers at a charge pressure of 3.0 MPa. Simulations reveal that both metallic and non-metallic cryocoolers exhibit similar variation patterns in cooling efficiency with frequency, showing an initial increase followed by a decrease, with peak COP occurring at 55 Hz. The non-metallic regenerator consistently demonstrates higher COP values than its metallic counterpart, indicating superior refrigeration performance.

The variation in COP originates from disparities in thermal penetration efficiency. At excessively low frequencies, insufficient thermal penetration reduces heat exchange efficiency. Higher frequencies shorten the refrigeration cycle duration, accelerating gas flow velocity through the regenerator. This increases gas-packing contact frequency per unit time; although individual contact duration may decrease, the cumulative heat transfer opportunity rises, improving heat exchange completeness and reducing corresponding losses. Concurrently, elevated frequency transitions flow regimes from laminar toward turbulent conditions, where enhanced fluid mixing reduces boundary layer thickness and dominates over increased dynamic pressure effects, ultimately decreasing flow resistance losses. Axial conduction loss remains stable as it primarily depends on axial temperature gradients, which show minimal sensitivity to frequency variations.

4.4 Comparison of Refrigeration Losses between Metallic-Packing and Non-Metallic Packing Regenerator Cryocoolers

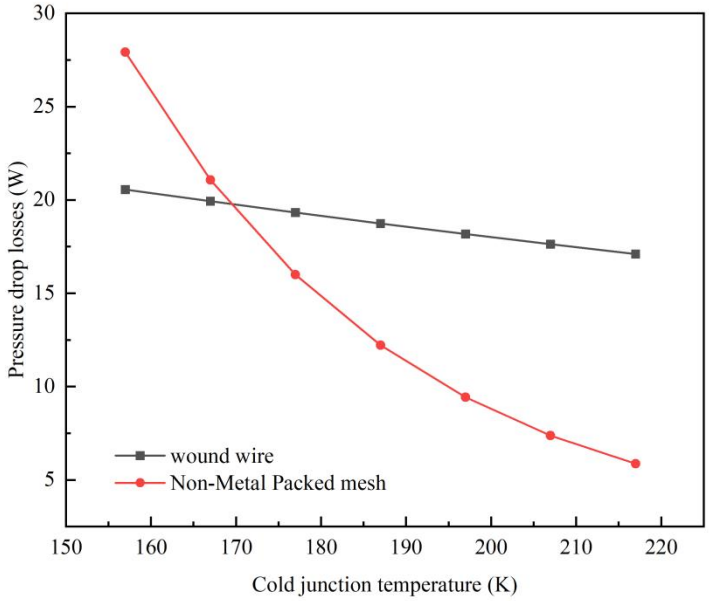

Figure 9 Comparison of Flow Resistance Losses in Stirling Cryocoolers with Metallic and Non - Metallic Regenerators at Different Temperatures

Figure 9 presents a comparison of flow resistance losses between metallic and non-metallic regenerator cryocoolers at different temperatures. The results show that as the cold-end temperature increases from 150K to 220K, the flow resistance losses of both metallic and non-metallic regenerator cryocoolers exhibit a decreasing trend. This is because at higher gas temperatures, the viscosity and density of the gas are relatively smaller, thereby reducing flow resistance. At lower cold-end temperatures, due to higher gas viscosity, both metallic and non-metallic regenerators show larger flow resistance losses. When the cold-end temperature is below 173K, the flow resistance of non-metallic regenerators exceeds that of metallic regenerators. At 160K, the flow resistance loss of the non-metallic material is 27W, while that of the metallic material is 20W. However, as the cold-end temperature rises, the flow resistance loss of the non-metallic material decreases more rapidly. When the cold-end temperature exceeds approximately 170K, its flow resistance loss becomes lower than that of the metallic material. At 220K, the flow resistance loss of the non-metallic material drops to about 6W, whereas the metallic material remains at approximately 18W. When the temperature exceeds 173K, the metallic surfaces exhibit higher roughness, while non-metallic materials typically have lighter weight and smoother surfaces, resulting in relatively smaller flow resistance and lower flow resistance losses. In conclusion, non-metallic regenerators demonstrate smaller internal losses and superior regenerative performance compared to metallic regenerators.

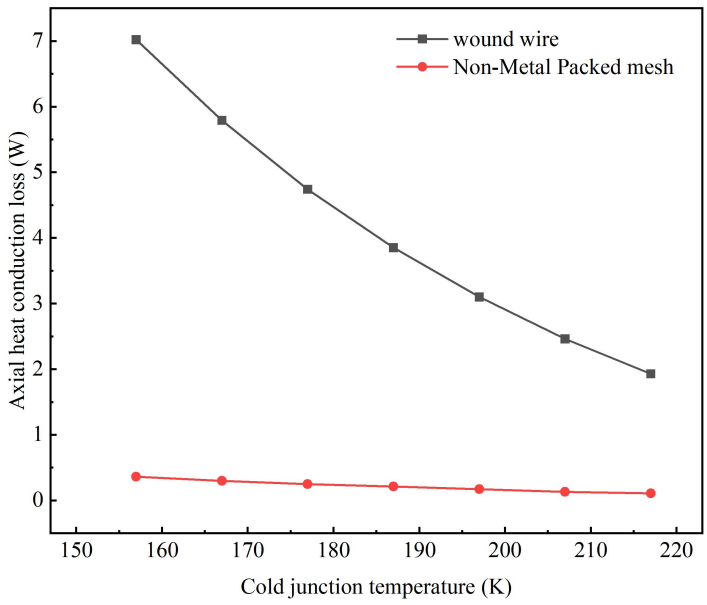

Figure 10 Comparison of Axial Heat Conduction Losses in Stirling Cryocoolers with Metallic And Non - Metallic

Regenerators at Different Temperatures

Figure 10 presents a comparison of axial conduction losses between metallic and non-metallic regenerator cryocoolers at different temperatures. The results show that as the cold-end temperature increases from 150K to 220K, the axial conduction loss of metallic regenerators decreases significantly, while that of non-metallic regenerators shows negligible variation. The reduction in metallic regenerator conduction loss is related to the decreased axial temperature gradient caused by the rising cold-end temperature. From the figure, it is evident that the axial conduction loss of metallic regenerators is significantly greater than that of non-metallic regenerators. During the operation of Stirling cryocoolers, distinct temperature gradients exist within the regenerators. Metallic materials inherently possess higher thermal conductivity compared to many non-metallic materials, enabling more efficient heat conduction. Additionally, since the spiral-wound wire mesh regenerator packing is integrally formed, there are no air gaps between metal wires as in stacked metal mesh configurations, which further exacerbates axial conduction. In the regenerator, when temperature gradients exist, the metal wire mesh rapidly transfers heat from high-temperature regions to low-temperature regions. Excessive axial conduction in regenerators adversely affects the performance of free-piston Stirling cryocoolers in multiple ways: Excessive axial conduction leads to excessive heat transfer along the axial direction, disrupting the temperature distribution between the hot and cold ends and reducing the regenerator's heat recovery efficiency. Furthermore, due to high axial conduction, the cryocooler requires additional energy consumption to maintain the low temperature at the cold end. This extra energy is not utilized for effective refrigeration but is wasted in compensating for the cold-end temperature rise caused by axial conduction, thereby negatively impacting refrigeration efficiency. Therefore, compared to non-metallic materials, the high axial conduction loss of metallic materials constitutes one of the primary defects of spiral-wound metallic regenerators.

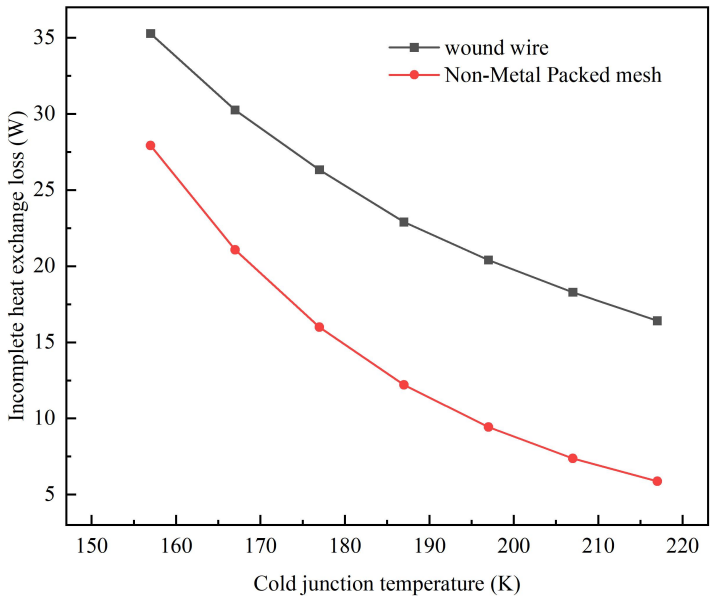

Figure 11 Comparison of Incomplete Heat Transfer Loss Losses in Stirling Cryocoolers with Metallic and non - Metallic Regenerators at Different Temperatures

Figure 11 presents a comparison of incomplete heat transfer losses between metallic and non-metallic regenerator cryocoolers at different temperatures. The results show that as the cold-end temperature rises from 150K to 220K, both metallic and non-metallic regenerator cryocoolers exhibit decreasing trends in incomplete heat transfer losses. This reduction correlates with the diminished temperature difference between the working gas and regenerator materials under elevated temperatures, which enhances heat exchange efficiency. At 150K, the incomplete heat transfer loss of the metallic regenerator measures 35W, compared to 28W for the non-metallic regenerator. When the cold-end temperature reaches 220K, these losses decrease to 17W and 6W for metallic and non-metallic regenerators respectively. Under identical cold-end temperatures, metallic regenerators consistently demonstrate higher incomplete heat transfer losses than non-metallic counterparts. The reduction magnitude of incomplete heat transfer losses in metallic regenerators is relatively smaller compared to non-metallic regenerators. The elevated incomplete heat transfer loss in metallic regenerators is directly related to their high axial conduction loss. The axial heat transfer disrupts the normal temperature distribution within the regenerator, leading to reduced temperature gradients during subsequent heat exchange processes. This diminished thermal gradient lowers heat transfer efficiency and thereby increases incomplete heat transfer losses.

4.4 Comparison of Refrigeration Performance between Metallic Packing and Non-Metallic Packing Regenerator Cryocoolers

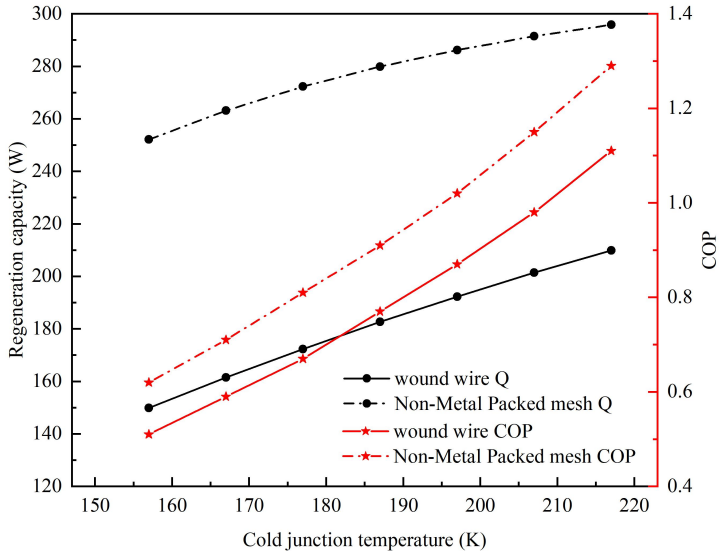

Figure 12 The Cooling Capacity and COP of the Cryocoolers with Metallic and Non-Metallic Regenerator under Different Cold End Temperatures

Figure 12 illustrates the refrigeration performance differences between metallic and non-metallic regenerator cryocoolers at various cold-end temperatures. At 187K operating temperature, the non-metallic regenerator cryocooler achieves 280W refrigeration capacity, whereas its metallic counterpart delivers only 180W under identical conditions. Concurrently, the non-metallic regenerator exhibits 0.2 higher COP and superior cooling efficiency, demonstrating better overall refrigeration performance. Comprehensive analysis confirms the non-metallic regenerator cryocooler outperforms the metallic version. The spiral-wound regenerator Stirling cryocooler maintains refrigeration capacity exceeding 150W with COP above 0.7 across the 180K temperature range, showing comparable efficiency to stacked metal mesh configurations at equivalent operating temperatures, making it an ideal cost-effective regenerator packing solution.

5 CONCLUSION

This chapter conducts numerical simulations based on a free-piston Stirling cryocooler prototype. A Sage model for the spiral-wound regenerator free-piston Stirling cryocooler was established with defined boundary conditions. Comparative simulations were performed on temperature field distribution, energy flow patterns, loss mechanisms, operational characteristics, and cooling efficiency between two regenerator material configurations. The full-scale Sage numerical model was developed based on the prototype, with parameter adjustments for metallic and non-metallic regenerators. Optimal packing parameters were determined through simulations: metallic regenerators achieved peak performance at 0.70 porosity with 70μm wire diameter, while non-metallic regenerators optimized at 55μm flow channel spacing and 20μm film thickness. Both configurations exhibited similar parametric trends, sharing optimal operating frequency (55Hz) and charge pressure (3.0MPa). Internal component losses increased with elevated charge pressure, though insufficient pressure (<2.6MPa) severely constrained cooling efficiency. While higher operating frequencies reduced internal losses, decreased displacer amplitude degraded refrigeration performance. At 187K operating temperature, the non-metallic regenerator delivered 280W refrigeration capacity versus 180W for the metallic counterpart, with a 0.2 higher COP and superior efficiency. Both configurations maintained COP values exceeding 0.7 across the operational temperature range. The spiral-wound regenerator design demonstrates promising refrigeration performance, providing new insights for developing cost-effective, high-efficiency Stirling cryocoolers with large cooling capacities.

COMPETING INTERESTS

The authors have no relevant financial or non-financial interests to disclose.

REFERENCE

[1] Getie M Z, Lanzetta F, Bégot S, et al. Reversed regenerative Stirling cycle machine for refrigeration application: A review. International Journal of Refrigeration, 2020, 118: 173–187. DOI: 10.1016/j.ijrefrig.2020.06.007.
[2] Wang B, Xu H, Zhang W Q, et al. Low-Temperature cryocoolers Based on Gas-Bearing Stirling Cryocoolers. Low Temperature and Superconductivity, 2017, 45(8): 26-31. DOI: 10.16711/j.1001-7100.2017.08.005.
[3] Liu S, Jiang Z, Ding L, et al, Impact of Operating Parameters on 80 K Pulse Tube Cryocoolers for Space Applications. International journal of refrigeration, 2019, 99: 226–233. DOI: 10.1016/j.ijrefrig.2018.12.026.
[4] Costa S C, Barreno I, Tutar M, et al. The thermal non-equilibrium porous media modelling for CFD study of woven wire matrix of a Stirling regenerator. Energy conversion and management, 2015, 89: 473-483. DOI: 10.1016/j.enconman.2014.10.019.
[5] Kim, Hong Seok, In Cheol Gwak, and Seong Hyuk Lee. Numerical Analysis of Heat Transfer Area Effect on Cooling Performance in Regenerator of Free-Piston Stirling Cooler. Case studies in thermal engineering, 2022, 32: 101875. DOI: 10.1016/j.csite.2022.101875.
[6] Cui Y, Qiao J, Song B, et al. Experimental study of a free piston Stirling cooler with wound wire mesh regenerator. Energy (Oxford), 2021, 23: 121287. DOI: 10.1016/j.energy.2021.121287.
[7] Zhu Haifeng, Yinong Wu, Na Li, et al. Experimental Study on Novel Regenerator Packing for Stirling Refrigerators. Proceedings of the 2015 Annual Academic Conference of the Shanghai Association of Refrigeration, Shanghai Association of Refrigeration, 2015.
[8] Cui Yunhao, Xiaotao Wang, Yanan Wang, et al. Simulation Study on the Application of Low-Cost Regenerator Packing in Liquid Nitrogen Temperature Range Stirling Refrigerators. Vacuum and Cryogenics, 2022, 28(3): 317–323. DOI: 10.3969/j.issn.1006-7086.2022.03.011.
[9] Cai Yachao. Study on Operational Characteristics of High-Capacity Integral Stirling Refrigerators. PhD dissertation, Zhejiang University, 2015.
[10] Gedeon D. Sage User's Guide: Stirling, Pulse-Tube and Low-T Cooler Model Classes. Gedeon Associates, 2014. https://refhub.elsevier.com/S1359-4311(19)38873-8/h0230.